

---

# Constrained Bayesian Optimization for Automatic Chemical Design

---

**Ryan-Rhys Griffiths**  
Department of Engineering  
University of Cambridge  
rrg27@cam.ac.uk

**José Miguel Hernández-Lobato**  
Department of Engineering  
University of Cambridge  
jmh233@cam.ac.uk

## Abstract

Automatic Chemical Design leverages recent advances in deep generative modelling to provide a framework for performing continuous optimization of molecular properties. Although the provision of a continuous representation for prospective lead drug candidates has opened the door to gradient-based optimization, some challenges remain for the design process. One known pathology is the model’s tendency to decode invalid molecular structures. The goal of this paper is to test the hypothesis that the origin of the pathology is rooted in the current formulation of Bayesian optimization. Recasting the optimization procedure as a constrained Bayesian optimization problem allows the model to produce novel drug compounds consistently ranked in the 100th percentile of the distribution over training set scores.

## 1 Introduction

The goal of chemical design is to find novel molecular structures that possess desirable properties. This search is complicated by the fact that chemical space is vast. From basic structural rules it is estimated that the space of pharmacologically active molecules satisfying Lipinski’s rule of five (Lipinski et al., 1997) is upwards of  $10^{60}$ , a novemdecillion (Reymond and Awale, 2012; Kirkpatrick and Ellis, 2004; Bohacek et al., 1996). Further to this, chemical space is discrete and so existing search methods in de novo drug design such as genetic algorithms cannot make use of continuous optimization techniques which use geometrical cues such as gradients to optimize the objective (Schneider and Fechner, 2005; Sliwoski et al., 2014). Recently, however, advances in deep generative modelling have produced models capable of interconverting between discrete and continuous representations of traditionally challenging data formats (Bowman et al., 2015). The generation of realistic synthetic samples from these models has found applications in image (Gregor et al., 2015), text (Bowman et al., 2015), speech and music (Oord et al., 2016) generation. Closely following this work, Gómez-Bombarelli et al. (Gómez-Bombarelli et al., 2016a) have developed a model capable of converting a discrete representation of molecules to and from a continuous representation. On conversion to the continuous representation, optimization that makes use of tools from continuous mathematics may be undertaken to search for molecules with desirable properties. Optimized continuous representations may then be generated from the model, giving rise to the concept of Automatic Chemical Design.

The operation of the Automatic Chemical Design pipeline is illustrated schematically in Figure 1. Starting with a discrete representation of some training molecules, denoted with feature 1 and feature 2, and a value for some design metric encoding drug-likeness, it is possible to construct a mathematical model of the space in-between these examples via Bayesian optimization. This statistical model is then used as the space to optimize over with the maxima being decoded as optimized discrete molecules. This approach has applications in high throughput virtual screening of drug candidates

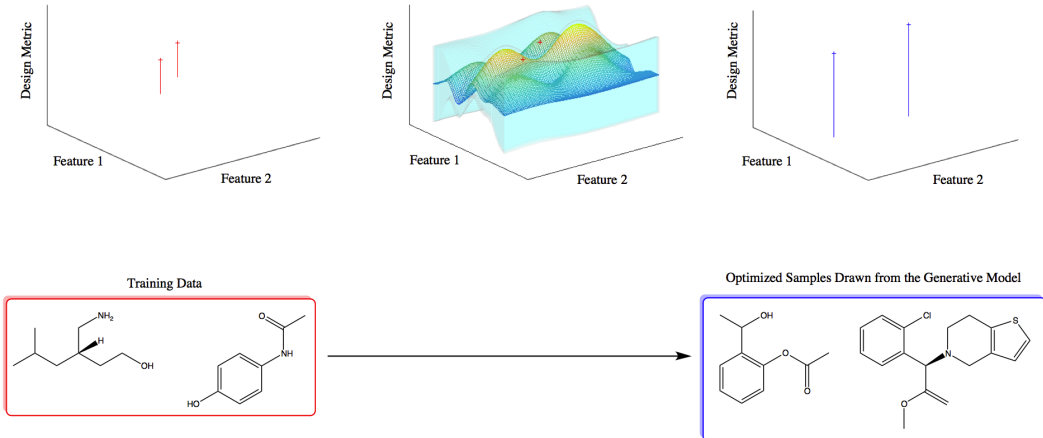


Figure 1: An Illustration of the Automatic Chemical Design Pipeline.

(Schneider, 2010; Pyzer-Knapp et al., 2015; Gómez-Bombarelli et al., 2016b) which may constitute a front end for more expensive molecular docking simulations or yet more expensive physical synthesis.

Although a strong proof of concept for the idea of performing continuous optimization in molecular space, the goal of *de novo* drug design using the Automatic Chemical Design model of (Gómez-Bombarelli et al., 2016a) faces some obstacles to realization:

1. Dead regions in the continuous latent space: How to ensure that the Bayesian Optimization procedure and the decoder operate in harmony?
2. What to optimize? How is it possible to encode the property of drug-likeness in a numerical metric?

These are the two questions this paper seeks to answer. The principle contribution of the paper, in section 4, will be to present a solution to the first question through the implementation of an algorithm for constrained Bayesian optimization. This will rein in the Bayesian optimization process such that it only selects points that lie within a certain region of the latent space where the probability of a successful decoding is high. The standalone question of how to increase the probability of a successful decoding has been addressed in recent work (Jaques et al., 2017; Janz et al., 2017). The second question will be addressed in section 5 from an applications perspective in terms of how best to go about using the model that addresses question 1. Section 2 presents the requisite theoretical background for understanding constrained Bayesian optimization while Section 3 illustrates the constrained Bayesian optimization setting using the toy example of the Branin-Hoo function.

## 2 Background

This section details the core aspects of the constrained Bayesian optimization problem and introduces the constrained acquisition function, expected improvement with constraints (EIC), used in all experiments reported. For a more in-depth introduction to Bayesian optimization the reader is referred to (Griffiths and Hernández-Lobato, 2017) and the references therein.

### 2.1 Constrained Bayesian Optimization

An extra dimension of complexity may be added to the formulation of the Bayesian optimization problem if regions of the design space are invalid. Examples of such situations occur in the optimization of Machine Learning algorithm hyperparameters where certain hyperparameter configurations can cause divergences in training or models to run out of memory. An example in chemistry would be the case where a region of chemical space corresponding to a set of similar drug compounds whose efficacy you are trying to evaluate are synthetically inaccessible. This class of problem is known as constrained Bayesian optimization within the Bayesian optimization framework. The constraint in

this case, is the property that regions of the design space are invalid. Typically, the constraint function will be boolean-valued. When such a constraint is known a priori, it may be incorporated into the optimization of the acquisition function. The more interesting case arises when the constraints are a priori unknown. The objective and constraint function may be unknown for two reasons:

1. The constraint has not been observed over the full design space and so it is necessary to interpolate and extrapolate the function values of inputs that have not yet been evaluated.
2. The constraint function may itself be noisy; multiple queries to the constraint function at the same input can result in different function values.

The same principles also apply to the unknown black-box objective function. Problems that adhere to the two points above come under the general class of stochastic programming problems ([Shapiro et al., 2014](#)). A natural goal for a statistical model of this kind of problem is to attempt to minimize the objective in expectation and to satisfy the constraints with high probability. Expressed formally the optimization problem is

$$\min_{\mathbf{x}} \mathbb{E}[f(\mathbf{x})] \text{ s.t. } \Pr(\mathcal{C}(\mathbf{x})) \geq 1 - \delta \quad (1)$$

where  $f(\mathbf{x})$  is the black-box objective function,  $\mathcal{C}(\mathbf{x})$  is the boolean function representing the constraint condition and  $1 - \delta$  is some user-specified minimum confidence that the constraint is satisfied ([Gelbart et al., 2014](#)). The requirement that the constraint be satisfied with high probability is a characteristic of Bayesian optimization problems with probabilistic constraints, a class of problems that describes the setting considered here. The black-box objective function is noisy because a single latent point may decode to multiple molecules when the model makes a mistake obtaining different values under the drug-likeness metric. The constraint is that a given latent point must decode successfully a large fraction of the times decoding is attempted. There is no valid estimate of the value of this fraction because in practice only a finite number of decodings are attempted. In such a fashion, the constraint can be considered to be noisy. The formulation of constrained Bayesian optimization given above can be extended to the case of multiple constraints ([Gelbart et al., 2014](#)).

## 2.2 Expected Improvement with Constraints

EIC may be thought of as expected improvement (EI) that offers improvement only when a set of constraints are satisfied. EIC was first introduced by ([Schonlau et al., 1998](#)) and has received more recent attention from ([Snoek, 2013](#); [Gardner et al., 2014](#)). It is defined as

$$\text{EIC}(\mathbf{x}) = \text{EI}(\mathbf{x}) \Pr(\mathcal{C}(\mathbf{x}) \geq 0) \quad (2)$$

where  $\Pr(\mathcal{C}(\mathbf{x}) \geq 0)$  denotes the probability that a boolean constraint  $\mathcal{C}(\mathbf{x})$  is satisfied. The implicit incumbent solution  $\eta$  suppressed in  $\text{EI}(\mathbf{x})$  in (2), may be set in an analogous way to vanilla expected improvement ([Gelbart, 2015](#)) as either:

1. The best observation in which all constraints are observed to be satisfied.
2. The minimum of the posterior mean such that all constraints are satisfied.

The latter approach is adopted for the experiments performed in this paper. If at the stage in the Bayesian optimization procedure where a feasible point has yet to be located, the form of acquisition function used is that defined by ([Gelbart, 2015](#)):

$$\text{EIC}(\mathbf{x}) = \begin{cases} \Pr(\mathcal{C}(\mathbf{x}) \geq 0) \text{EI}(\mathbf{x}), & \text{if } \exists \mathbf{x}, \Pr(\mathcal{C}(\mathbf{x}) \geq 1 - \delta) \\ \Pr(\mathcal{C}(\mathbf{x}) \geq 0), & \text{otherwise} \end{cases} \quad (3)$$

The intuition behind (3) is that if the probabilistic constraint is violated everywhere, the acquisition function selects the point having the highest probability of lying in the feasible region. The algorithm ignores the objective until it has located the feasible region.

### 3 Experiment I: The Branin-Hoo Function

The Branin-Hoo function will act as a toy problem on which to test the validity of the custom algorithmic implementation for constrained Bayesian optimization. The optimization of the Branin-Hoo function has long been a benchmark for the comparison of global optimization algorithms (Dixon and Szegö, 1978) and more recently has become a benchmark for the comparison of Bayesian optimization algorithms (Eggensperger et al., 2013). The particular variant of the Branin-Hoo optimization of interest here is the constrained formulation of the problem featured in (Gelbart et al., 2014). The 2D Branin-Hoo function is given as

$$f(\mathbf{x}) = \left( x_2 - 5.1 \frac{x_1^2}{4\pi^2} + 5 \frac{x_1}{\pi} - 6 \right)^2 + 10 \left( 1 - \frac{1}{8\pi} \right) \cos(x_1) + 10 \quad (4)$$

and has three global minima at the coordinates  $(-\pi, 12.275)$ ,  $(\pi, 2.275)$  and  $(9.42478, 2.475)$ . In order to formulate the problem as a constrained optimization problem, a disk constraint on the region of feasible solutions,

$$(x_1 - 2.5)^2 + (x_2 - 7.5)^2 \leq 50, \quad (5)$$

is introduced. In contrast to the formulation of the problem in (Gelbart et al., 2014), the disk constraint is coupled in this scenario in the sense that the objective and the constraint will be evaluated jointly at each iteration of Bayesian optimization. In addition, the observations of the black-box objective function will be assumed to be non-noisy. The minima of the Branin-Hoo function as well as the disk constraint are illustrated in Figure 2.

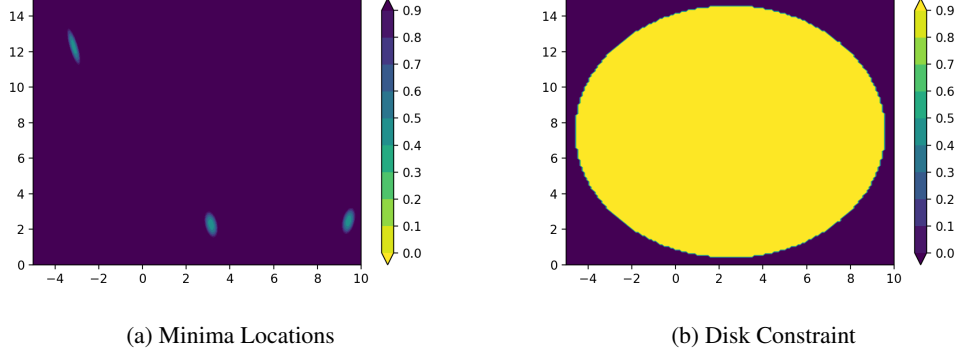


Figure 2: Constrained Bayesian optimization of the 2D Branin-Hoo Function.

The disk constraint eliminates the upper-left and lower-right solutions, leaving a unique global minimum at  $(\pi, 2.275)$ . Given that the implementation of constrained Bayesian optimization considered here relies on the use of a sparse GP as the underlying statistical model of the black-box objective and as such is designed for scale as opposed to performance, the results will not be compared directly against those of Gelbart et al. (Gelbart et al., 2014) who use a full GP to model the objective. It will be sufficient to compare the performance of the algorithm against random sampling. Both the sequential Bayesian optimization algorithm and the parallel implementation utilising the Kriging-Believer algorithm will be tested.

#### 3.1 Implementation

A Sparse GP featuring the FITC approximation, based on the implementation of (Bui et al., 2016) is used to model the black-box objective function. The kernel choice is exponentiated quadratic with ARD lengthscales. The number of inducing points  $M$  was chosen to be 20 in the case of sequential Bayesian optimization, and 5 in the case of parallel Bayesian optimization using the Kriging-Believer

algorithm. The sparse GP is trained for 400 epochs using Adam (Kingma and Ba, 2014) with the default parameters and a learning rate of 0.005. The minibatch size is chosen to be 5. The extent of jitter, a parameter that provides stabilization in the computation of the posterior predictive distribution such that the Cholesky decomposition will not fail (Rasmussen and Williams, 2006), is chosen to be 0.00001. A Bayesian Neural Network (BNN), adapted from the MNIST digit classification network of (Hernández-Lobato et al., 2016) is trained using black-box alpha divergence minimization to model the constraint.

The network has a single hidden layer with 50 hidden units, Gaussian activation functions and logistic output units. The mean parameters of  $q$ , the approximation to the true posterior, are initialized by sampling from a zero-mean Gaussian with variance  $\frac{2}{d_{\text{in}} + d_{\text{out}}}$  according to the method of (Glorot and Bengio, 2010), where  $d_{\text{in}}$  is the dimension of the previous layer in the network and  $d_{\text{out}}$  is the dimension of the next layer in the network. The value of  $\alpha$  is taken to be 0.5, minibatch sizes are taken to be 10 and 50 Monte Carlo samples are used to approximate the expectations with respect to  $q$  in each minibatch. The BNN adapted from (Hernández-Lobato et al., 2016) was implemented in the Theano library (Bastien et al., 2012; Team et al., 2016). The LBGs method (Liu and Nocedal, 1989) was used to optimize the EIC acquisition function in all experiments.

### 3.2 Results

The results of the sequential constrained Bayesian optimization algorithm with EIC are shown in Figure 3. The algorithm was initialized with 50 labeled data points drawn uniformly at random from the grid depicted. 40 iterations of Bayesian optimization were carried out.

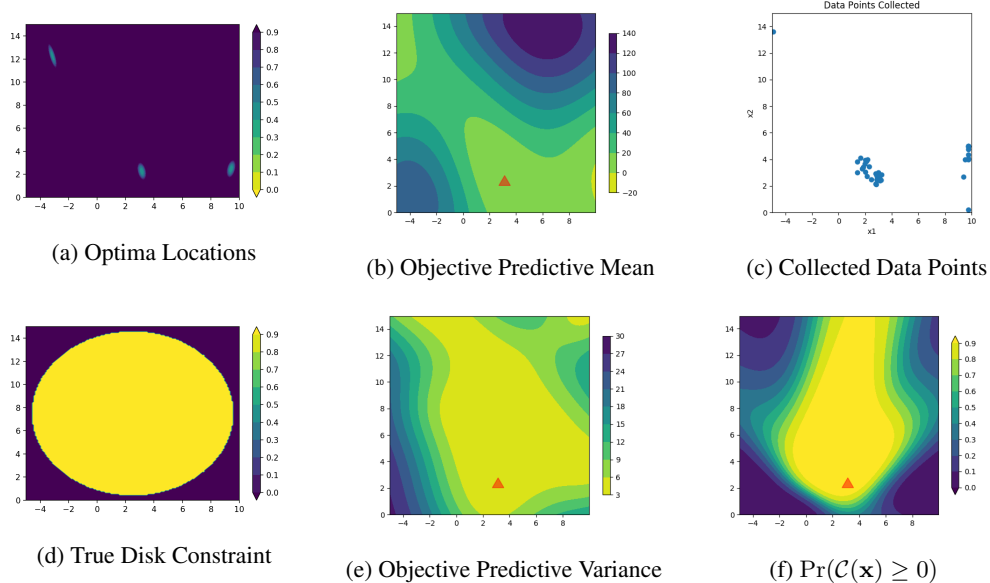


Figure 3: Constrained Bayesian Optimization on the 2D Branin-Hoo Function with a Coupled Disk Constraint. **a)** Minima of the true Branin-Hoo function. **b)** Contour plot of the predictive mean of the sparse GP used to model the objective function. Lighter colours indicate lower values of the objective. **c)** Data points collected over 40 iterations of sequential Bayesian optimization. **d)** The disk constraint, where the feasible region is given in yellow. **e)** The predictive variance of the sparse GP used to model the objective function. **f)** The contour learned by the BNN giving the probability of constraint satisfaction.

The figures are provided for illustrative purposes only and show that the algorithm is correctly managing to collect data in the vicinity of the single feasible minimum. Figure 4 compares the performance of parallel Bayesian optimization using the Kriging-Believer algorithm against the results of random sampling. Both algorithms were initialized using 10 data points drawn uniformly at random from the grid on which the Branin-Hoo function is defined and were run for 10 iterations of Bayesian optimization. At each iteration a batch of 5 data points was collected for evaluation.

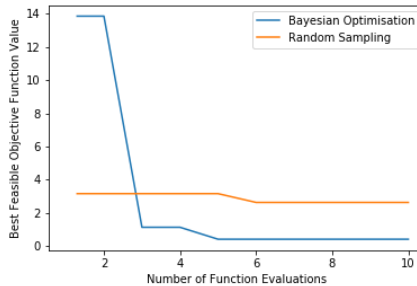


Figure 4: Performance of Parallel Bayesian Optimization with EIC against Random Sampling.

After 10 iterations, the minimum feasible value of the objective function was 0.42 for parallel Bayesian optimization with EIC using the Kriging-Believer algorithm and 2.63 for random sampling. The true minimum feasible value is 0.40. It is worth noting that these results are not statistically significant and are merely provided as a means of demonstrating that the implementation is taking the constraint into account.

### 3.3 Discussion

The results above act as a proof of concept that the implementation of constrained Bayesian optimization is behaving as expected in so far as it recognises the constraint in the problem and appears to do better than random sampling. It could be worth performing some investigation into how much worse the sparse GP performs relative to the full GP in the constrained setting. Another aspect that could be explored is the impact of the initialization. It has recently been argued that different algorithms will vary in their performance depending on how much information about the design space there is available (Morar et al., 2017).

## 4 Experiment II: Automatic Chemical Design

This section constitutes the formal test of the hypothesis from (Gómez-Bombarelli et al., 2016a) that the root cause of the decoder’s lack of efficiency in decoding latent points collected by Bayesian optimization arises as a result of the presence of large “dead regions” in the latent space from which it becomes difficult to decode valid molecules. The section will proceed firstly by describing the implementation details of the Bayesian optimization procedure for the molecular dataset.

Secondly, the results of a set of diagnostic experiments are presented. The experiments are diagnostic in the sense that they are designed to investigate the hypothesis that unconstrained Bayesian optimization is collecting points in a dead region that lies far away from the training data in the latent space. Thirdly, the performance of constrained Bayesian optimization will be compared directly with that of the Bayesian optimization procedure of the original model (baseline model) in terms of the number of valid and drug-like molecules generated. The related aspect of the number of new molecules generated will also be discussed here. Lastly the quality of the molecules produced by constrained Bayesian optimization and the baseline model is compared. Quality in this case is measured by the objective function scores of new molecules proposed by the methods. The objective function is

$$J^{\text{QED}}(m) = \text{QED}(m) - \text{SA}(m) - \text{ring-penalty}(m). \quad (6)$$

in all experiments reported, where  $m$  denotes a molecule,  $\text{QED}(m)$  is the quantitative estimate of drug-likeness for that molecule (Bickerton et al., 2012) and  $\text{SA}(m)$  is its synthetic accessibility (Ertl and Schuffenhauer, 2009). The ring penalty term is the same as that featured in (Gómez-Bombarelli et al., 2016a).

## 4.1 Implementation

The implementation details of the encoder-decoder network remain unchanged from (Gómez-Bombarelli et al., 2016a). The objective function is modelled by a sparse GP based on the FITC approximation in the case of both constrained and unconstrained Bayesian optimization.  $M$ , the number of inducing points is set to 500, the minibatch size is 5000, the number of training epochs is 50 and the learning rate is 0.005. If unmentioned, the remaining parameters remain the same as in the case of the implementation for the Branin-Hoo function. In the case of the constrained Bayesian optimization algorithm, the BNN is constructed with 2 hidden layers each 100 units wide with ReLU activation functions and a logistic output. Minibatch size is set to 1000 and the network is trained for 5 epochs with a learning rate of 0.0005.

Again, if unmentioned all remaining parameters are unchanged from the implementation for the Branin-Hoo experiments. In both the unconstrained and constrained Bayesian optimization procedures, 20 iterations of parallel Bayesian optimization were performed using the Kriging-Believer algorithm, collecting data in batch sizes of size 50. Both the unconstrained and constrained approaches were initialized with 249,456 training points corresponding to 249,456 drug-like molecules drawn at random from the ZINC database (Irwin et al., 2012). The same training set of randomly-drawn molecules as (Gómez-Bombarelli et al., 2016a) was used. The train/test split of this data was in the ratio of 90/10. In results where the mean and standard error is reported, each run corresponds to a different random train/test split in the ratio of 90/10. For constrained Bayesian optimization, the binary classification BNN was trained using a balanced training set of 234,880 latent points with binary labels. The labelling procedure for these 234,880 latent points was motivated by the diagnostic experiments outlined in the following section.

## 4.2 Diagnostic Experiments and Labelling Criteria

A set of experiments were designed in order to investigate the hypothesis that points collected by Bayesian optimization lie far away from the training data in latent space and hence give rise to a large number of invalid decodings. Five sets of latent points were created. The first set consisted of 50 latent points from the training data. In the very small noise (VS) set, 1% noise was added to 50 randomly chosen training values along each dimension. The percentage of noise in this case is defined relative to the maximum difference between training set values along a given dimension. The noise itself is drawn from a uniform distribution that ranges from  $[-\%noise, +\%noise]$ . In the small noise (S) set 10% noise was added to the training values along each dimension. In the big noise (B) set 50% noise was added to the training values along each dimension. The final set, (BO), consisted of 50 points collected by running the Bayesian optimization procedure of the original model. These latent points subsequently underwent 500 decode attempts and the resulting observations are summarized in Figure 5.

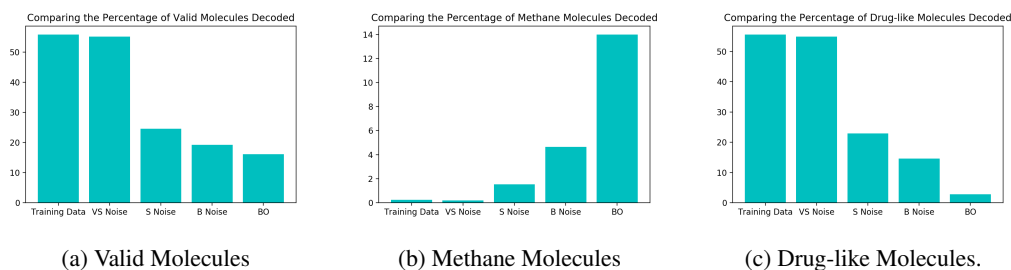


Figure 5: Experiments on 5 disjoint sets comprising 50 latent points each. VS Noise are training data points with approximately 1% noise added to their values, S Noise have 10% noise added to their values and B Noise have 50% noise added to their values. As an example, the percentage noise in the case of 1% noise is defined to be a value drawn from a uniform distribution where the lower end of the range is 0.01 times the maximum difference between the values of the training data along a given dimension. **a)** The percentage of times a given latent point from each set was decoded to a valid molecule, averaged over 50 latent points. **b)** The percentage of times a given latent point from each set was decoded to a methane molecule, averaged over 50 latent points. **c)** The percentage of times a given latent point from each set was decoded to a drug-like molecule, averaged over 50 latent points .

There would appear to be a noticeable decrease in the percentage of valid molecules decoded as one moves further away from the training data in latent space (adding more noise to the training values should be equivalent to moving further away from them). Consequently, the fact that the points collected by Bayesian optimization do the worst in terms of their percentage of valid decodings would suggest that these points lie farther away from the training data than even the B Noise set. A further artefact of the decoder is that it would seem to over-generate methane molecules when far away from the data. One hypothesis for why this is the case is that methane is represented as 'C' in the SMILES syntax and is by far the most common character. Hence far away from the training data, combinations such as 'C' followed by a stop character may have high probability under the distribution over sequences learned by the decoder. Given that methane has far too low a molecular weight (or equivalently its SMILES is too short) to be a suitable drug candidate, a third plot is generated in [Figure 5c](#), whereupon the percentage of decoded molecules is given such that the molecules are both valid and have a tangible molecular weight. From here on in the definition of a tangible molecular weight will be interpreted somewhat arbitrarily as being a SMILES length of 5 or greater. Further to this, molecules that are both valid and have a SMILES length greater than 5 will be referred to as drug-like.

From the histogram in [Figure 5c](#), it may be observed that the points collected by Bayesian optimization produce an even smaller proportion of drug-like molecules than they do valid molecules relative to the training and noise-displaced training data. As a result of these diagnostic experiments, it was decided that the criteria for labelling latent points to initialize the binary classification neural network for the constraint would be the following: if the latent point decodes into drug-like molecules in more than 20% of decode attempts, it should be classified as a positive class and negative otherwise. The results of the constrained Bayesian optimization procedure trained using the aforementioned labelled data will be presented in the following section.

### 4.3 Molecular Validity

As mentioned in the section on implementation, the constraint function was initialized with 117,440 positive class points and 117,440 negative class points. For a latent point to be labelled positive at least 20% of its attempted decodings must be valid. The positive labelled data points were obtained by running the training data through the decoder and classifying those points that satisfied the criteria as positive. The negative class points, in contrast, were collected by decoding points sampled uniformly at random across the design space. The relative performance of constrained Bayesian optimization and unconstrained Bayesian optimization (baseline) ([Gómez-Bombarelli et al., 2016a](#)) is compared in [Figure 6a](#).

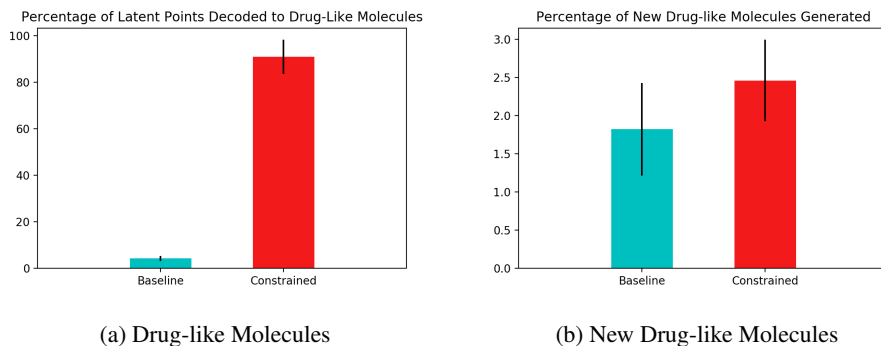


**Figure 6: a)** The percentage of latent points decoded to drug-like molecules. 20 iterations of Bayesian optimization with batches of 50 data points collected at each iteration (1000 latent points decoded in total). The standard error is given for 5 separate train/test set splits of 90/10. Drug-like in this instance specifies a requirement that the molecules must both be valid and have a length greater than 5 in the SMILES Representation. **b)** The percentage of new drug-like molecules generated from 20 iterations of Bayesian optimization with batches of 50 data points collected at each iteration (1000 latent points decoded in total). The standard error is given for 5 separate train/test set splits of 90/10.

For this experiment, each latent point undergoes 100 decoding attempts and the most probable SMILES string is retained. This SMILES string is then categorised as being drug-like or not drug-like.

The results suggest that greater than 80% of the latent points decoded by constrained Bayesian optimization produce drug-like molecules compared to less than 5% for unconstrained Bayesian optimization. However, one must also account for the fact that the constrained approach may be gaining an artificial advantage on this metric by decoding the training data. There would seem to be a fine line between exploring the latent space and wandering into a dead region. If the constrained region is too tight, then the decoding process will tend to produce molecules that have been seen in training, yet when there is no constraint, there is a danger that the optimization process will decode points in dead regions of latent space. One means of controlling the trade-off between these two extremes would be to treat the  $\delta$  parameter in (1) as a parameter to be tuned. If the threshold  $\delta$ , the minimum percentage of decodings required to be drug-like, is more lenient, the noose around the training data is loosened but one will be less successful at decoding due to the risk of entering a dead region of the latent space. Conversely, if the noose is too tight, most of the molecules decoded are liable to be training data. One means of controlling the balance between these two factors is to look at the number of new drug-like molecules generated by the process. Constrained and unconstrained Bayesian optimization are compared on this metric in [Figure 6b](#).

One may observe that constrained Bayesian optimization outperforms unconstrained Bayesian optimization in terms of generating new molecules, but not by a large margin. The number of new drug-like molecules however is a metric that is subject to some abuse due to the arbitrary definition of what it means to be drug-like. Following a manual inspection of the SMILES strings collected by the unconstrained optimization approach, it would appear as though there were many strings with lengths marginally larger than the cutoff point, which is suggestive of partially decoded molecules. As such, a fairer metric for comparison that is in-keeping with the ethos of Bayesian optimization should be the quality of the new molecules produced as judged by the scores from the black-box objective function. This comparison is made in the following section.

#### 4.4 Molecular Quality

The histogram in [Figure 7](#) represents the distribution of objective function scores seen in the training data. The blue and red lines are respectively the best molecules produced by unconstrained Bayesian optimization and constrained Bayesian optimization averaged over 5 random train/test splits.

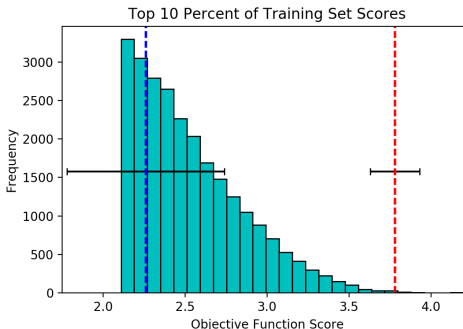


[Figure 7](#): The best scores for new molecules generated from the baseline model (blue) and the model with constrained Bayesian Optimization (red). The vertical lines show the best scores averaged over 5 separate train/test set splits of 90/10. The histogram is presented such that only the top 10% of the training data scores are depicted.

[Table 1a](#) gives the percentile that the averaged score of the new molecules found by each process occupies in the distribution over training set scores.

Returning briefly to the results of [Figure 7](#), constrained Bayesian optimization would appear to be able to generate higher quality molecules relative to unconstrained Bayesian optimization and in slightly higher quantity. In order to ensure that the averaged results aren't vulnerable to outliers, the scores of the best new drug-like molecules are provided in [Table 1b](#).

Over the 5 runs undertaken, the constrained optimization procedure in every run produced new drug-like molecules in the 100th percentile of the distribution over training set scores. Given a set of drug-like molecules, being able to generate new candidates that rank in the 100th percentile in the

Run	Baseline	Constrained
1	49th	86th
2	51st	97th
3	12th	90th
4	37th	93rd
5	29th	94th

(a) Average Percentile Score of New Molecules

Run	Baseline	Constrained
1	88th	100th
2	98th	100th
3	76th	100th
4	96th	100th
5	95th	100th

(b) Percentile Score of Single Best Molecule

Table 1: **a)** Percentile of the Averaged New Molecule Score Relative to the Training Data. **b)** Percentile of the Best New Molecule Score Relative to the Training Data. The Results of 5 Separate Train/Test Set Splits of 90/10 are Provided in Both Cases.

distribution over training set scores is an enticing prospect. There is however, one caveat in that it is first necessary to know what score to optimize. In drug discovery, the question of what constitutes a drug-like molecule is a surprisingly difficult question to think about (Bickerton et al., 2012). The following section will address questions related to knowing what to optimize and will propose some areas of application for the current model.

## 5 Objective Function Design

Given that the gold standard for validating metrics such as SA and QED, as featured in (6), is agreement with human medicinal chemists, one proposal for the model of Automatic Chemical Design would be to make it available in the fashion described by (Brochu et al., 2010). In this manner human medicinal chemists could be used to help provide a prior over the likely or desirable parameter settings for the objective function that is being sought. One can envisage an iterative process occurring whereby a human chemist accepts or rejects the model’s proposal based on chemical intuition, the model updates the coefficients of the objective it is trying to optimize and proposes another molecule that is hopefully closer to what the chemist is looking for. Further considerations involving conflicts between different metrics are described in (Griffiths and Hernández-Lobato, 2017).

## 6 Conclusion and Future Work

### 6.1 Contributions

The reformulation of the search procedure in the Automatic Chemical Design model as a constrained Bayesian optimization problem has led to concrete improvements on two fronts:

1. Validity - The number of valid molecules produced by the constrained optimization procedure offers a marked improvement over the original model. Additionally, it may be possible to treat the criteria for defining the constraint as a tuneable parameter that controls the extent of exploration of the latent space.
2. Quality - For five independent train/test splits, the scores of the best molecules generated by the constrained optimization procedure consistently ranked in the 100th percentile of the distribution over training set scores. The ability to find new molecules that are competitive with the very best of the training set is a powerful demonstration of the model’s capabilities. As a further point, the generality of the approach should be emphasised. This approach is liable to work for a large range of objectives encoding countless desirable molecular properties.

### 6.2 Future Work

Future work may entail experiments to investigate if further performance gains can be achieved by tuning the criteria for defining a constraint. Furthermore, it would be interesting to investigate the possibility of developing an interface whereby a human medicinal chemist could interact with the model directly in order to perform Bayesian optimization in a hierarchical fashion in the design of the objective function as well as in the design of molecules that optimize it.

## References

Christopher A Lipinski, Franco Lombardo, Beryl W Dominy, and Paul J Feeney. Experimental and computational approaches to estimate solubility and permeability in drug discovery and development settings. *Advanced drug delivery reviews*, 23(1-3):3–25, 1997.

Jean-Louis Reymond and Mahendra Awale. Exploring chemical space for drug discovery using the chemical universe database. *ACS chemical neuroscience*, 3(9):649–657, 2012.

Peter Kirkpatrick and Clare Ellis. Chemical space. *Nature*, 432(7019):823, 2004.

Regine S Bohacek, Colin McMartin, and Wayne C Guida. The art and practice of structure-based drug design: A molecular modeling perspective. *Medicinal research reviews*, 16(1):3–50, 1996.

Gisbert Schneider and Uli Fechner. Computer-based de novo design of drug-like molecules. *Nature reviews. Drug discovery*, 4(8):649, 2005.

Gregory Sliwoski, Sandeepkumar Kothiwale, Jens Meiler, and Edward W Lowe. Computational methods in drug discovery. *Pharmacological reviews*, 66(1):334–395, 2014.

Samuel R Bowman, Luke Vilnis, Oriol Vinyals, Andrew M Dai, Rafal Jozefowicz, and Samy Bengio. Generating sentences from a continuous space. *arXiv preprint arXiv:1511.06349*, 2015.

Karol Gregor, Ivo Danihelka, Alex Graves, Danilo Jimenez Rezende, and Daan Wierstra. Draw: A recurrent neural network for image generation. *arXiv preprint arXiv:1502.04623*, 2015.

Aaron van den Oord, Sander Dieleman, Heiga Zen, Karen Simonyan, Oriol Vinyals, Alex Graves, Nal Kalchbrenner, Andrew Senior, and Koray Kavukcuoglu. Wavenet: A generative model for raw audio. *arXiv preprint arXiv:1609.03499*, 2016.

Rafael Gómez-Bombarelli, David Duvenaud, José Miguel Hernández-Lobato, Jorge Aguilera-Iparraguirre, Timothy D Hirzel, Ryan P Adams, and Alán Aspuru-Guzik. Automatic chemical design using a data-driven continuous representation of molecules. *arXiv preprint arXiv:1610.02415*, 2016a.

Gisbert Schneider. Virtual screening: an endless staircase? *Nature reviews. Drug discovery*, 9(4):273, 2010.

Edward O Pyzer-Knapp, Changwon Suh, Rafael Gómez-Bombarelli, Jorge Aguilera-Iparraguirre, and Alán Aspuru-Guzik. What is high-throughput virtual screening? a perspective from organic materials discovery. *Annual Review of Materials Research*, 45:195–216, 2015.

Rafael Gómez-Bombarelli, Jorge Aguilera-Iparraguirre, Timothy D Hirzel, David Duvenaud, Dougal Maclaurin, Martin A Blood-Forsythe, Hyun Sik Chae, Markus Einzinger, Dong-Gwang Ha, Tony Wu, et al. Design of efficient molecular organic light-emitting diodes by a high-throughput virtual screening and experimental approach. *Nature materials*, 15(10):1120–1127, 2016b.

Natasha Jaques, Shixiang Gu, Dzmitry Bahdanau, José Miguel Hernández-Lobato, Richard E. Turner, and Douglas Eck. Sequence tutor: Conservative fine-tuning of sequence generation models with KL-control. In Doina Precup and Yee Whye Teh, editors, *Proceedings of the 34th International Conference on Machine Learning*, volume 70 of *Proceedings of Machine Learning Research*, pages 1645–1654, International Convention Centre, Sydney, Australia, 06–11 Aug 2017. PMLR. URL <http://proceedings.mlr.press/v70/jaques17a.html>.

David Janz, Jos van der Westhuizen, and José Miguel Hernández-Lobato. Actively learning what makes a discrete sequence valid. *arXiv preprint arXiv:1708.04465*, 2017.

Ryan-Rhys Griffiths and José Miguel Hernández-Lobato. Constrained bayesian optimization for automatic chemical design. *arXiv preprint arXiv:1709.05501*, 2017.

Alexander Shapiro, Darinka Dentcheva, and Andrzej Ruszczynski. *Lectures on Stochastic Programming: Modeling and Theory, Second Edition*. Society for Industrial and Applied Mathematics, Philadelphia, PA, USA, 2014. ISBN 1611973422, 9781611973426.

Michael A Gelbart, Jasper Snoek, and Ryan P Adams. Bayesian optimization with unknown constraints. *arXiv preprint arXiv:1403.5607*, 2014.

Matthias Schonlau, William J Welch, and Donald R Jones. Global versus local search in constrained optimization of computer models. *Lecture Notes-Monograph Series*, pages 11–25, 1998.

Jasper Snoek. *Bayesian optimization and semiparametric models with applications to assistive technology*. PhD thesis, University of Toronto, 2013.

Jacob Gardner, Matt Kusner, Kilian Q Weinberger, John Cunningham, and Zhixiang Xu. Bayesian optimization with inequality constraints. In *Proceedings of the 31st International Conference on Machine Learning (ICML-14)*, pages 937–945, 2014.

Michael Adam Gelbart. *Constrained Bayesian Optimization and Applications*. PhD thesis, Harvard University, 2015.

Laurence Charles Ward Dixon and Giorgio P Szegö. *Towards global optimisation*. North-Holland Amsterdam, 1978.

K. Eggensperger, M. Feurer, F. Hutter, J. Bergstra, J. Snoek, H. Hoos, and K. Leyton-Brown. Towards an empirical foundation for assessing bayesian optimization of hyperparameters. In *NIPS workshop on Bayesian Optimization in Theory and Practice*, 2013.

Thang D Bui, Josiah Yan, and Richard E Turner. A unifying framework for sparse gaussian process approximation using power expectation propagation. *arXiv preprint arXiv:1605.07066*, 2016.

Diederik Kingma and Jimmy Ba. Adam: A method for stochastic optimization. *arXiv preprint arXiv:1412.6980*, 2014.

C. E. Rasmussen and C. K. I. Williams. *Gaussian Processes for Machine Learning*. MIT Press, 2006.

José Miguel Hernández-Lobato, Yingzhen Li, Mark Rowland, Daniel Hernández-Lobato, Thang D Bui, and Richard E Turner. Black-box  $\alpha$ -divergence minimization. In *Proceedings of the 33rd International Conference on International Conference on Machine Learning-Volume 48*, pages 1511–1520. JMLR. org, 2016.

Xavier Glorot and Yoshua Bengio. Understanding the difficulty of training deep feedforward neural networks. In *Proceedings of the Thirteenth International Conference on Artificial Intelligence and Statistics*, pages 249–256, 2010.

Frédéric Bastien, Pascal Lamblin, Razvan Pascanu, James Bergstra, Ian Goodfellow, Arnaud Bergeron, Nicolas Bouchard, David Warde-Farley, and Yoshua Bengio. Theano: new features and speed improvements. *arXiv preprint arXiv:1211.5590*, 2012.

The Theano Development Team, Rami Al-Rfou, Guillaume Alain, Amjad Almahairi, Christof Angermueller, Dzmitry Bahdanau, Nicolas Ballas, Frédéric Bastien, Justin Bayer, Anatoly Belikov, et al. Theano: A python framework for fast computation of mathematical expressions. *arXiv preprint arXiv:1605.02688*, 2016.

Dong C Liu and Jorge Nocedal. On the limited memory bfgs method for large scale optimization. *Mathematical programming*, 45(1):503–528, 1989.

Marius Tudor Morar, Joshua Knowles, and Sandra Sampaio. *Initialization of Bayesian Optimization Viewed as Part of a Larger Algorithm Portfolio*. 5 2017.

John J Irwin, Teague Sterling, Michael M Mysinger, Erin S Bolstad, and Ryan G Coleman. Zinc: a free tool to discover chemistry for biology. *Journal of chemical information and modeling*, 52(7):1757–1768, 2012.

G Richard Bickerton, Gaia V Paolini, Jérémie Besnard, Sorel Muresan, and Andrew L Hopkins. Quantifying the chemical beauty of drugs. *Nature chemistry*, 4(2):90–98, 2012.

Peter Ertl and Ansgar Schuffenhauer. Estimation of synthetic accessibility score of drug-like molecules based on molecular complexity and fragment contributions. *Journal of cheminformatics*, 1(1):8, 2009.

Eric Brochu, Tyson Brochu, and Nando de Freitas. A bayesian interactive optimization approach to procedural animation design. In *Proceedings of the 2010 ACM SIGGRAPH/Eurographics Symposium on Computer Animation*, pages 103–112. Eurographics Association, 2010.